

# Characterization and Isolation of Ductular Cells Coexpressing Neural Cell Adhesion Molecule and Bcl-2 from Primary Cholangiopathies and Ductal Plate Malformations

Luca Fabris,<sup>\*,†</sup> Mario Strazzabosco,<sup>†</sup> Heather A. Crosby,<sup>‡</sup> Giorgio Ballardini,<sup>§</sup> Stefan G. Hubscher,<sup>¶</sup> Deirdre A. Kelly,<sup>||</sup> James M. Neuberger,<sup>\*</sup> Alastair J. Strain,<sup>‡</sup> and Ruth Joplin<sup>\*</sup>

From the Liver Research Laboratories,<sup>\*</sup> Department of Medicine, School of Biochemistry,<sup>‡</sup> and the Department of Pathology,<sup>¶</sup> Children's Hospital,<sup>||</sup> University Hospital, Birmingham, United Kingdom; the Department of Medical and Surgical Sciences,<sup>†</sup> Clinica Medica I, Università di Padova, Padova, Italy; and the Istituto di Clinica Medica II,<sup>§</sup> Policlinico S. Orsola, Università di Bologna, Bologna, Italy

**It has recently been shown that reactive bile ductules display neuroendocrine features, including immunoreactivity for the neural cell adhesion molecule (NCAM). In this study we have compared the immunohistochemical expression of NCAM with that of HEA-125 (biliary specific) and LKM-1 (hepatocyte specific) and other markers relevant to morphogenesis (Bcl-2, EMA) and cell proliferation (Ki-67) in cryostat sections from different chronic liver diseases and from fetal livers at different gestational ages. In parallel, viable NCAM-positive ductular cells were purified from collagenase digests of cirrhotic livers by immunomagnetic separation and characterized by immunocytochemistry and transmission electron microscopy. We demonstrated that reactive ductules with atypical morphology coexpressed NCAM and Bcl-2 and were found mainly in congenital diseases associated with ductal plate malformation and in primary cholangiopathies. On the contrary, reactive ductules with typical morphology were negative for NCAM/Bcl-2 and positive for EMA. Reactive ductules coexpressing NCAM/Bcl-2 were negative for the proliferation marker Ki-67 and appeared to be directly connected with periportal hepatocytes. In fetal livers NCAM/Bcl-2 was transiently expressed during the early developmental stages of ductal plate (10–16 weeks) and started to disappear as the ductal plate began duplicating. NCAM-positive ductal plate cells were Ki-67 negative, becoming positive in duplicated segments. Thus the histogenesis of ductular reactive cells seems to recapitulate the early stages of biliary ontogenesis. In primary cholangiopathies and ductal**

**plate malformations, these cells do not appear to mature further, and thus abundant ductular structures coexist with vanishing mature ducts. These NCAM-positive ductular cells were immunopurified from patients with chronic cholestatic liver diseases and showed ultrastructural features consistent with a less differentiated phenotype than mature cholangiocytes. These isolated cells represent a useful model for *in vitro* studies. (Am J Pathol 2000, 156:1599–1612)**

A common histopathological response to many forms of chronic liver diseases is an increase in the number of bile duct-like structures,<sup>1–3</sup> paralleled by an inflammatory cell infiltrate and periportal fibrosis. This ductular reaction is thought to act as a pacemaker in the development of the progressive fibrotic process that leads to liver cirrhosis.<sup>1,3,4</sup> After liver damage, bile ductular cells produce a number of mediators, such as interleukin-6,<sup>5,6</sup> transforming growth factor- $\beta$ ,<sup>7</sup> endothelin-1,<sup>8</sup> monocyte chemoattractant protein-1,<sup>9</sup> platelet-derived growth factor,<sup>10</sup> tumor necrosis factor- $\alpha$ ,<sup>11</sup> nitric oxide,<sup>12</sup> and parathyroid hormone-related peptide,<sup>13</sup> which is probably involved in paracrine communications with mesenchymal and inflammatory cells.

Currently, four types of ductular reaction are described: typical, atypical, cholangiolar, and oval cell.<sup>14,15</sup> Atypical ductular reaction is characterized by an anastomosing network of ductules, with poorly defined lumina, lined by flattened cells with a scant cytoplasm; atypical ductules are most often localized at the peripheral zone of the portal space. This occurs in most forms of chronic cholestatic liver injury, such as in primary biliary cirrhosis (PBC), primary sclerosing cholangitis (PSC), and chronic extrahepatic biliary obstruction. Available data indicate that whereas typical reactive ductules derive from proliferating

---

Supported by grants from the Children's Liver Diseases Foundation (to H.A.C.), Endowment Fund of United Birmingham Hospitals (to J.M.N. and R.J.), and from Telethon (Grants E-430 and E-873) and Cofinanziamento MURST 1998 (Grant 9806210866) (to L.F. and M.S.).

Accepted for publication January 12, 2000.

Address reprint requests to Dr. Mario Strazzabosco, Department of Medical and Surgical Sciences, Clinica Medica I, Via Giustiniani, 2, 35128 Padova, Italy. E-mail: mstrazza@ux1.unipd.it.

eration of the preexisting well-differentiated biliary epithelial cells,<sup>16</sup> atypical ductules arise from ductular metaplasia of hepatocytes<sup>14,17</sup> and/or from activation of a facultative bipotential stem cell,<sup>14,18</sup> the actual identity of which in humans has not yet been determined. These cells, capable of differentiating into biliary epithelial cells and hepatocytes, are thought to be located in close proximity to the terminal bile ductules and to sustain liver regeneration under conditions such as fulminant hepatic failure that compromise the proliferative capability of hepatocytes and cholangiocytes.

The study of the biological characteristics of reactive ductular cells may lead to a better understanding of both the dynamics of epithelial cell populations in the liver and some basic liver pathophysiological mechanisms. The phenotypic profile of ductular cells has been partly characterized by histological studies: they are anchored on a basement membrane and can express major histocompatibility complex (MHC) class I proteins<sup>19,20</sup> and cell adhesion molecules, such as carcinoembryonic antigen<sup>21</sup> and intercellular adhesion molecule-1.<sup>22,23</sup> Furthermore, recent data indicate that reactive ductules display neuroendocrine features, including immunoreactivity for chromogranin A and for the neural cell adhesion molecule (NCAM).<sup>24</sup> NCAM is a surface glycoprotein, belonging to the immunoglobulin superfamily, that mediates cell-cell (homophilic) and cell-matrix (heterophilic) interactions during the development of the nervous system,<sup>25–28</sup> lung, and gut epithelia.<sup>29</sup>

Given the role played by NCAM in morphogenetic processes, we have investigated its immunohistochemical expression and that of a number of markers relevant to morphogenesis and cell proliferation on the biliary epithelium in a wide variety of chronic hepatobiliary diseases and in fetal livers at different gestational ages. In particular, the B-cell leukemia lymphoma-2 protein (Bcl-2), a protooncogene product localized to the mitochondrial inner membrane,<sup>30</sup> is of potential interest: its ability to block apoptosis is required in the developmental processes of new epithelial structures.<sup>31,32</sup> Our results indicate that in congenital diseases related to ductal plate malformation and primary diseases of the biliary tree, atypical ductules retain less differentiated immunophenotypic features, such as coexpression of NCAM and Bcl-2, similar to those transiently expressed during the embryonic development of the biliary system. Furthermore, based on a positive selection of cells expressing NCAM, we have devised a method to purify a viable population of atypical ductular cells from cirrhotic human liver; ultrastructural studies of these isolated cells further support the less differentiated biliary phenotypic traits of NCAM-positive cells.

## Materials and Methods

### Immunohistochemistry

#### Source of Tissue

Human tissue samples from hepatectomy specimens were snap frozen in liquid nitrogen and stored at  $-70^{\circ}\text{C}$ .

Normal liver tissue ( $n = 10$ ) was obtained from graft reductions for pediatric liver transplant recipients. Diseased liver tissue was obtained at the time of the orthotopic liver transplantation; this included parenchymal liver cirrhosis (chronic autoimmune hepatitis,  $n = 5$ ; cryptogenic cirrhosis,  $n = 5$ ; alcoholic liver cirrhosis,  $n = 5$ ), primary immune-mediated cholangiopathies (PBC,  $n = 12$ ; PSC,  $n = 8$ ), and congenital cholangiopathies (extrahepatic bile duct atresia,  $n = 5$ ), congenital diseases of bile ducts related to ductal plate malformation (Caroli's disease,  $n = 2$ ; polycystic liver disease,  $n = 2$ ). Diagnosis was made by clinical, serological, and histological criteria. Fetal livers ( $n = 10$ ) from human embryos and fetuses from the 10th to 16th weeks of gestation were obtained, after informed consent, from legal voluntary abortions.

### Classification of Intrahepatic Bile Ducts

In adult livers, intrahepatic biliary epithelium was categorized according to the method of Ludwig.<sup>33</sup> Major ducts were accompanied by a hepatic artery branch and comprised both interlobular ducts (luminal diameter between 50 and 100  $\mu\text{m}$ , lined by cuboidal cells) and septal ducts (luminal diameter greater than 100  $\mu\text{m}$ , lined by a columnar epithelium). Bile ductules were the smallest conduits (less than 50  $\mu\text{m}$  in diameter), were lined by cuboidal epithelial cells, and were not accompanied by the small branches of portal vein and hepatic artery. Typical or atypical reactive ductules were respectively classified according to the following histological criteria: lumen patency (discernible or no discernible lumen), morphology of the lining epithelium (cuboidal or flattened), and ductule profile (well-formed or irregular anastomosing plexuses).

In fetal livers development of biliary epithelium was categorized as reported by Van Eyken<sup>34</sup> and Shah.<sup>35</sup> During the early stages of embryonic development (from 6 to 8 weeks), hepatoblasts adjacent to mesenchyme around the largest portal vein branches close to the liver hilum alter their phenotype toward bile duct-type cells, giving rise to the primordial ductal plate (9–10th weeks).

### Alkaline Phosphatase Immunostaining

Serial 5- $\mu\text{m}$  cryostat sections were fixed in acetone at room temperature, and immunohistochemistry was performed by the alkaline phosphatase method, using monoclonal antibodies against human epithelial antigen-125 (HEA-125), NCAM, epithelial membrane antigen (EMA), and B-cell leukemia lymphoma-2 protein (Bcl-2) (see also Table 1). The working dilution of each antibody was determined in preliminary tests. After preliminary blocking with normal rabbit serum (1:10; Dako), sections were incubated with primary antibodies for 1 hour at room temperature. After incubation with the primary antibody, sections were washed three times before incubation with rabbit anti-mouse immunoglobulins (1:25; Dako) for 45 minutes. After further washing, sections were incubated with alkaline phosphatase mouse anti-alkaline phosphatase (APAAP) (1:50; Dako) for 45 minutes. Antibody bind-

**Table 1.** Primary Antibodies Used for Immunohistochemistry and Biological Significance of the Corresponding Markers

Markers	Source	Isotype	Optimal dilution	Biological significance
HEA-125	Progen Biotechnik GmbH	IgG1 (mouse)	1:100 (APAAP) 1:50 (IF)	34-kd epithelial surface glycoprotein (egp34) biliary lineage-specific <sup>42</sup> homologous to nidogen <sup>72</sup>
NCAM	Dako	IgG2a (mouse)	1:20 (APAAP) 1:10 (IF)	Family of cell surface sialoglycoproteins mediating homophilic and heterophilic interactions in neuroectodermally derived tissues <sup>25-28</sup>
EMA	Dako	IgG2a (mouse)	1:20 (APAAP) 1:10 (IF)	Group of 250–400-kd glycosylated membrane proteins, present in a variety of epithelia of both normal and neoplastic tissues <sup>73</sup> ; a late biliary maturation marker <sup>57</sup>
Bcl-2	Dako	IgG1 (mouse)	1:40 (APAAP) 1:20 (IF)	Protein localized to the mitochondrial inner membrane, able to block apoptosis <sup>30</sup> ; it is up-regulated in processes requiring protection from apoptosis, such as metaplasia <sup>63,64</sup>
Ki-67	Immunotech (MIB-1 clone)	IgG2a (mouse)	1:40 (IF)	Nuclear antigen associated with the cell cycle, expressed throughout all phases except G <sub>0</sub> <sup>36</sup>
LKM-1	See references <sup>38,39</sup>	IgG (human) FITC-conjugated	Neat (IF)	P450IID6, a cytochrome P-450 monooxygenase localized to the smooth endoplasmic reticulum; hepatocyte-specific <sup>40,41</sup>

ing was detected using fast red substrate (Sigma Chemical Co., Poole, UK), and sections were counterstained with Mayer's hematoxylin (Sigma). In controls, primary antibody was omitted. The sections were assessed by three independent observers (LF, RJ, SGH) according to the classification based on bile duct morphology given above.

#### Double Immunostaining

Double immunostaining was performed on selected sections with different combinations of the following antibodies (see Table 1): HEA-125, NCAM, EMA, Bcl-2, and Ki-67 (MIB-1 clone, a nuclear antigen associated with the cell cycle),<sup>36</sup> and Texas red and fluorescein isothiocyanate (FITC) (anti-IgG1 or anti-IgG2a, 1:50; Europath, Bude, UK) conjugates as secondary fluorescent antibodies. When primary antibodies belonged to different subclasses (such as HEA-125 and NCAM, HEA-125 and EMA, HEA-125 and Ki-67, NCAM and Bcl-2) conventional simultaneous labeling could be used: the two primary antibodies were mixed, incubated together for 30 minutes, and then visualized with a mixture of Texas red and FITC conjugates. When primary antibodies shared the same subclass (such as HEA-125 and Bcl-2, NCAM and EMA, NCAM and Ki-67), staining was performed using the reverse sequential indirect method, in which the sequence of addition of primary antibodies in duplicate immunostaining experiments is reversed.<sup>37</sup> FITC-conjugated human IgG from a liver kidney microsome-1 (LKM-1)-positive patient (0.1 mg/ml in phosphate-buffered saline (PBS)) was used as a hepatocellular marker, because it homogeneously and specifically decorates the hepatocyte smooth endoplasmic reticulum by reacting with a cytochrome P-450 monooxygenase isoform.<sup>38-41</sup> LKM-1 was used in combination with HEA-125<sup>42</sup> and NCAM,<sup>24</sup> taken as biliary cell markers. Sections were mounted in Diazabicyclo(2.2.2)octane (DABCO) to retard the fading of the fluorochromes. In

controls reactivity of each conjugate with each primary antibody was tested to exclude the possibility of subclass cross-reactivity.

Sections were analyzed by with a laser scanning confocal microscopy MCR-500 system, equipped with a krypton-argon laser (Bio-Rad), for coincident sites of reactivity. Fluorescence images were collected and analyzed in the dual-channel mode, with the laser lines at 488 and 568 nm. Under these conditions, single labeling appears red (Texas red) and green (FITC), whereas coincident labeling appears yellow. To measure the relative fluorescence intensity of antigen expression on reactive ductules, the fluorescence within a defined area occupied by biliary ductular cells was defined in bands of increasing intensity (from 0 to 255), where the highest values were shown in red (219–255) and the lowest appeared in blue (37–72); intensity below 36 was black and indicated unstained areas.

#### Isolation of NCAM-Positive Ductular Cells from Human Liver

##### Source of Tissue

Normal liver ( $n = 12$ ) from the pediatric segmental transplantation procedures and cirrhotic liver ( $n = 12$ ) from patients undergoing liver transplantation for PBC ( $n = 9$ ) and PSC ( $n = 3$ ) were used for cell isolation studies. Donor organs, perfused with University of Wisconsin surgical preservation fluid, and slices of cirrhotic liver, in tissue culture medium, were stored for up to 24 hours at 4°C before cell preparation.

##### Purification of Cells

Approximately 30 g of liver tissue was dissected, finely diced, and incubated at 37°C with 50 ml collagenase type 1A (1 mg/ml; Sigma Chemical Company). After 1–2

hours of incubation the digest was filtered through fine mesh (Sigma screen cup; Sigma Chemical Company), and the filtered tissue pieces were further diced to enhance the release of cells. Digested tissue pieces and filtrate were recombined and incubated for an additional 30 minutes to 1 hour at 37°C. After a total of 2–3 hours of digestion the tissue pieces were again filtered through fine mesh and the filtrate was washed three times in PBS. After the final wash the volume of filtrate was adjusted to 24 ml. Three milliliters of filtrate was overlaid on Percoll gradients, each composed of 3.5 ml 1.04 g/ml Percoll underlaid by 3.5 ml 1.09 g/ml Percoll and then centrifuged at  $800 \times g$  for 30 minutes at room temperature. After centrifugation, five separate fractions were evident. Each fraction was harvested separately, washed three times in PBS, and centrifuged at  $800 \times g$  for 30 minutes. Cell smears from the final cell pellet derived from each fraction were stained with the biliary specific HEA-125 and cytokeratin 19 (CK-19) antibodies, to establish where atypical cholangiocytes could be harvested. In addition, from each fraction, cells were immunopurified using HEA-125 as already described<sup>43,44</sup> and further characterized by immunocytochemistry for CK-19, NCAM, and EMA. The supernatant and pellicle (fraction 1) that floated as a layer on top of the gradient were composed mainly of cell debris and hepatocytes. Some HEA-125/CK-19-positive cells were present, but cells in this fraction had very low viability (<20%). Cells equilibrating in 1.04 g/ml Percoll (fraction 2) and as a layer on top of 1.09 g/ml Percoll (fraction 3) were composed of single cells and cell aggregates, which were positive for HEA-125 and CK-19 and were >95% viable. In particular, fraction 2 was composed of single cells or small aggregates of 2–10 cells each. All were positive for CK-19 and, in cirrhotic liver, many (>50%) were positive for NCAM and negative for EMA. In contrast, HEA-125-positive cells equilibrating in fraction 3 were predominantly small to large aggregates of around 10–100 cells each. These cells were positive for CK-19 and EMA (>95% positive) but were largely negative for NCAM (<5% positive). Very few cells were present in 1.09 g/ml Percoll (fraction 4), whereas the pellet (fraction 5) appeared to be composed predominantly of erythrocytes. These preliminary studies indicate that atypical ductular cells fractionate predominantly in 1.04 g/ml Percoll, whereas mature cholangiocytes pass through this fraction and can be harvested from the layer of cells floating on 1.09 g/ml Percoll. Therefore, fractions 2 and 3 were pooled together for further sequential immunomagnetic separation of biliary cells expressing NCAM and HEA-125. Pooled fractions 2 and 3 were incubated with anti-NCAM (37°C for 30 minutes) followed by bead-conjugated rat anti-mouse IgG2 (DynaL, Oslo, Norway) (4°C for 30 minutes). After magnetic harvest of NCAM-positive cells, a subset of biliary epithelial cells was purified from the NCAM-negative population by immunomagnetic separation using HEA-125, as previously reported.<sup>43,44</sup> The two purified biliary epithelial cell populations (NCAM-positive versus NCAM-negative, respectively) were characterized for immunocytochemistry and transmission electron microscopy (TEM).

### Characterization of Purified Cells

**Immunostaining:** Smears of freshly isolated cells were immunostained with anti-HEA-125 (1:10), anti-CK19 (1:50, IgG2a isotype; Dako), anti-NCAM (1:10), and anti-EMA (1:50) monoclonal antibodies. Sites of primary antibody binding were visualized with sheep anti-mouse IgG2a (CK19, NCAM and EMA) conjugated to FITC (1:50). In controls primary antibody was omitted. Cells were counterstained with propidium iodide.

**Transmission Electron Microscopy:** After they were washed three times, purified cells were resuspended in 1 ml of PBS in 1.5-ml Eppendorf tubes. Magnetic beads and attached cells were concentrated for 2 minutes, using a Dynal multiEppendorf magnetic particle concentrator (DynaL). Once the cells had concentrated, PBS was replaced with 1 ml of 2.5% glutaraldehyde in 0.1 mol/L cacodylate buffer for 2 hours. Without removing the tubes from the magnet, so as not to disturb the concentrated cells, the fixed cells were washed gently three times in cacodylate buffer, osmicated in 1% OsO<sub>4</sub> for 4 hours, dehydrated through graded alcohols, and embedded in Epon resin. Sections showing gold interference color (approximately 70 nm) were cut and mounted on Formvar/carbon-coated slot grids. They were stained with uranyl acetate and lead citrate and were examined using a Jeol 100× TEM.

## Results

### Immunohistochemistry

#### Normal Livers

Distribution of HEA-125, EMA, NCAM, and Bcl-2 alkaline phosphatase immunostaining in normal liver tissue is summarized in Table 2

In normal livers HEA-125 was specific for biliary epithelium, being expressed on bile ductules and major ducts, but not in hepatocytes and other nonparenchymal cells. EMA was homogeneously expressed on the apical aspect of cholangiocytes in both major ducts and ductules. In sections that were double stained for HEA-125 and EMA, coincident labeling between the two antigens was present in major ducts as well as in smaller ductules (not shown). The biliary epithelium was always negative for NCAM; by double labeling with HEA-125, NCAM-positive structures could be seen along the portal tract and surrounding the bile ducts, most likely representing nerve fibers (not shown). Bcl-2 also failed to stain the biliary epithelium but was positive in isolated lymphocytes (not shown). The proliferation marker Ki-67 was sporadically positive only in some scattered hepatocytes (not shown). LKM-1 stained homogeneously the hepatocyte cytoplasm, as previously reported.<sup>38–41</sup>

#### Fetal Livers

The results of the immunostaining in fetal liver are shown in Figure 1. In fetal livers from 10–12 weeks of gestation (Figure 1a), ie, during the early stages of bile



**Table 2.** Distribution of HEA-125, EMA, NCAM, and Bcl-2 on Biliary Epithelium in Normal and Diseased Liver Tissue

	HEA 125	EMA	NCAM	Bcl-2
Normal liver				
Ductules	+	+	-	-
Ducts	+	+	-	-
Parenchymal liver cirrhosis				
Typical reactive ductules	+	+	-	-
Atypical reactive ductules	+	-	±	±
Ducts	+	+	-	-
Primary immune-mediated cholangiopathies				
Typical reactive ductules	+	+	-	-
Atypical reactive ductules	+	-	+	+
Ducts	+	+	-	-
Congenital cholangiopathies				
Typical reactive ductules	+	+	-	-
Atypical reactive ductules	+	-	+	+
Ducts	+	+	-	-
Ductal plate malformations				
Typical reactive ductules	+	+	-	-
Atypical reactive ductules	+	-	+	+
Ducts	+	+	-	-

On major ducts and typical reactive ductules scattered NCAM- and Bcl-2-positive cells can be seen occasionally. Staining key: strong (+, >50% ducts/ductules positive; weak (±), 10–50% ducts/ductules positive; absent (-), < 10% ducts/ductules positive.

duct development, NCAM was positive in most cells forming the single-layered ductal plates surrounding a large portal vein branch. As the ductal plate developed and the single layer was duplicated by a second layer (14 weeks of gestation, Figure 1b), NCAM immunoreactivity began to disappear from those segments in which a lumen could be recognized and started incorporating into mesenchyma (16 weeks of gestation, Figure 1c). In contrast, EMA was never seen on single-layered ductal plates and gave a faint staining only in the duplicated segments forming tubular structures (not shown). Double immunostaining using NCAM (Texas Red conjugate) and Bcl-2 (FITC) demonstrated that NCAM-positive cells forming a ductal plate also expressed Bcl-2, as shown by dismerged images (Figure 1d). These cells were also positive for HEA-125. Finally, NCAM-positive ductal plate cells (Texas Red conjugate) showed no evidence of active proliferation, as judged by the negative double immunolabeling with Ki-67 (FITC) (not shown). A widespread, strong Ki-67 expression was instead noticed on the surrounding parenchymal and hemopoietic cells. These findings indicate that NCAM and Bcl-2 positivity identifies immature biliary cells at an early and transient developmental stage, which is also characterized by a low rate of proliferation. A focal positivity for Ki-67 could be observed in NCAM-negative cells lining bile ducts with a clear tubular morphology.

### Diseased Livers

The results of the immunostaining in a variety of chronic liver diseases are reported in Table 2. NCAM and EMA immunoreactivity was compared to the biliary epithelial cell marker HEA-125 (Figure 2a–f); whereas HEA-

125 homogeneously stained all biliary epithelial structures (Figure 2, a and d), EMA and NCAM showed an inverse pattern of distribution, similar to that reported above for fetal livers. EMA (Figure 2, b and e) was positive in major ducts and typical ductules that were negative for NCAM, whereas NCAM (Figure 2, c and f) was consistently positive in ductules with atypical morphology that were negative for EMA.

As in fetal livers, confocal analysis revealed that NCAM-positive biliary cells were also positive for Bcl-2. NCAM and Bcl-2 expression on biliary epithelial cells was coincident, not only in terms of distribution, but even in the intensity of binding, as shown by a color banding analysis of the images (Figure 3a). Major ducts and typical ductules, showing focal NCAM/Bcl-2 double positive cells, were observed only occasionally (5–10%) (not shown).

As shown in Figure 3, b–f, atypical ductular cells co-expressing NCAM and Bcl-2 were seen particularly in immune-mediated cholangiopathies (PBC and PSC), in biliary atresia, and in congenital diseases related to ductal plate malformations (Caroli's disease, polycystic liver disease). In a number of cases representative of the range of liver diseases studied (biliary atresia: *n* = 2; PBC: *n* = 2; PSC: *n* = 1; cryptogenic cirrhosis: *n* = 2; autoimmune hepatitis: *n* = 1; alcoholic cirrhosis: *n* = 1), we calculated the ductular area positive for NCAM as a percentage of the total ductular area recognized by HEA-125. As summarized in Table 3, the most extensive immunoreactivity for NCAM was found in biliary atresia and PBC; in PSC the proportion of NCAM-positive ductules was still higher than in cryptogenic cirrhosis, alcoholic cirrhosis, and autoimmune hepatitis. It is noteworthy that whereas in cholestatic liver diseases NCAM and Bcl-2-

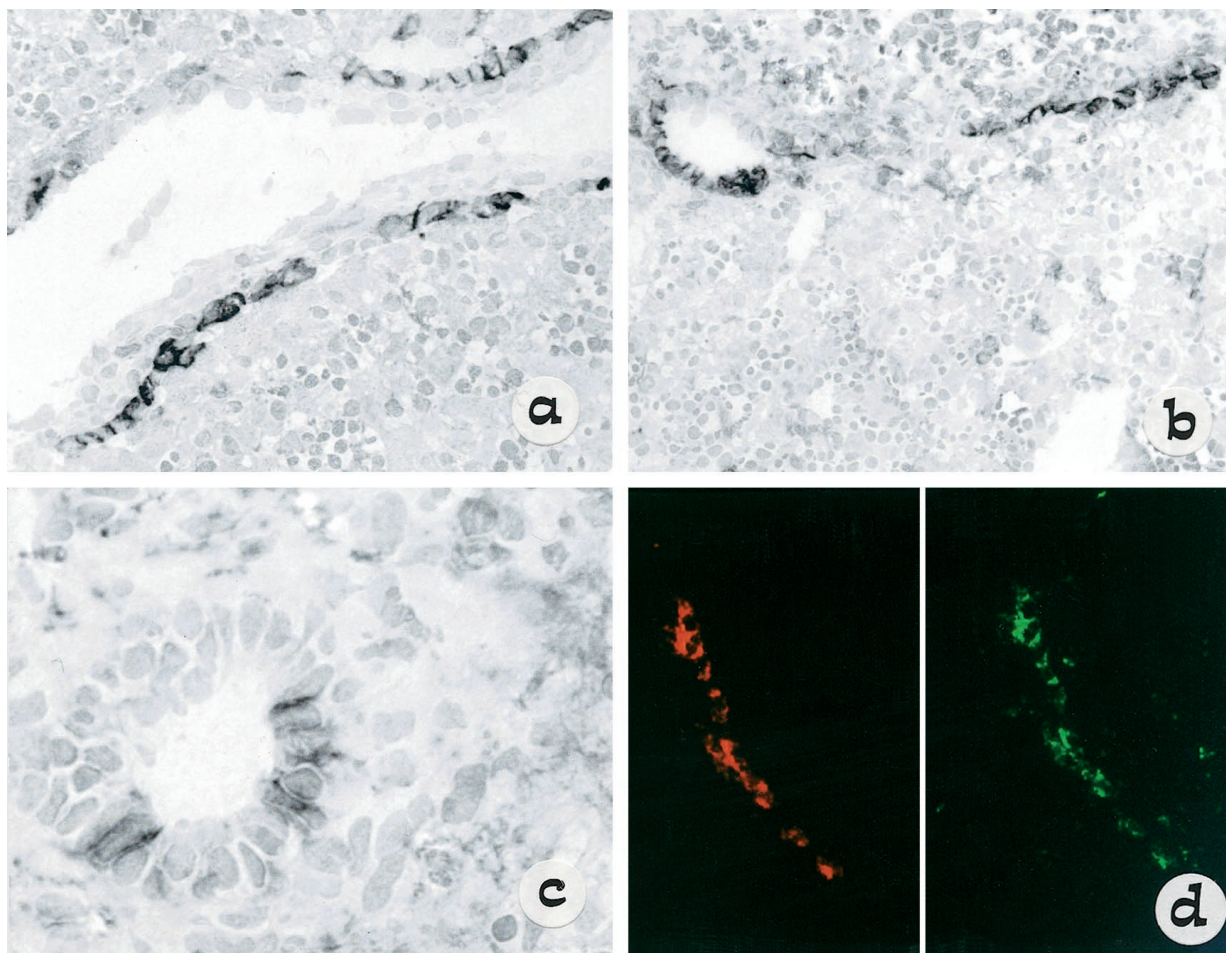


**Figure 1.** Light micrograph of single staining (immunoperoxidase method) showing the distribution of NCAM during the early steps in bile duct morphogenesis (**a–c**). An indirect three-step immunoperoxidase technique was used with peroxidase-labeled rabbit anti-mouse and swine anti-rabbit immunoglobulin (Dako) and diaminobenzidine substrate. NCAM is expressed on a single-layer ductal plate surrounding a large portal vein branch, as seen in fetal liver at 12 weeks' gestation (**a**: original magnification,  $\times 60$ ). However, NCAM is disappearing as duplicated segments are formed with staining still present in residual ductal plate remnants, as seen in fetal liver at 14 weeks' gestation (**b**: original magnification,  $\times 40$ ). Faint patchy NCAM staining is observed in bile ducts with an easily recognizable lumen incorporating into mesenchyma, as seen in fetal liver at 16 weeks' gestation (**c**: original magnification,  $\times 120$ ). In **d** the high level of colocalization between NCAM (red) and Bcl-2 (green) is demonstrated in developing ductal plate by dismerged images of double staining at confocal analysis.

positive atypical ductules were present both at the center and at the margin of portal tracts (Figure 3, c–f, yellow), in parenchymal liver cirrhosis NCAM and Bcl-2 coincident staining was restricted to a small proportion of ductules, at the margin between the regenerative hepatocyte nodule and the fibrous septa (Figure 3b, yellow).

The proliferation activity of NCAM-positive ductular cells was investigated by double immunostaining with NCAM and Ki-67. A range of liver diseases was studied (biliary atresia:  $n = 2$ ; Caroli's disease:  $n = 1$ ; polycystic liver disease:  $n = 1$ ; PBC:  $n = 3$ ; PSC:  $n = 2$ ; cryptogenic cirrhosis:  $n = 1$ ; autoimmune hepatitis:  $n = 1$ ; alcoholic cirrhosis:  $n = 1$ ). Whereas Ki-67-positive periportal hepatocytes were frequently found, NCAM/Ki-67-positive cells were a very rare finding (not shown). These data indicate that NCAM-positive atypical ductules are not actively proliferating.

To study the histological relationship between hepatocytes and NCAM-positive cholangiocytes, double immunostaining for the biliary markers NCAM or HEA-125 and the hepatocellular marker LKM-1 was performed for a

range of liver diseases (Caroli's disease:  $n = 2$ ; polycystic liver disease:  $n = 2$ ; PBC:  $n = 4$ ; PSC:  $n = 1$ , cryptogenic cirrhosis:  $n = 3$ ; autoimmune hepatitis:  $n = 2$ ; alcoholic cirrhosis:  $n = 3$ ). In all types of liver diseases studied, NCAM-positive cholangiocytes (red) formed periportal sprouting cords organized into irregularly shaped and poorly formed ductules that directly anastomosed with periseptal LKM-1-positive hepatocytes (Figure 4a, green). Double labeling of NCAM with LKM-1 revealed no sites of NCAM coexpression on the plasma membrane of LKM-1-positive hepatocytes; however, some discrete intracytoplasmic granules positive for NCAM could be observed in periseptal hepatocytes that were positive for LKM-1. In contrast, double labeling for HEA-125 (red) and LKM-1 (green) showed that periportal hepatocytes, which were negative for NCAM, as judged in serial consecutive sections (Figure 4b), began to express HEA-125 plasma membrane immunoreactivity (Figure 4c, yellow). This finding was most commonly observed in parenchymal liver cirrhosis, particularly in alcoholic liver disease.



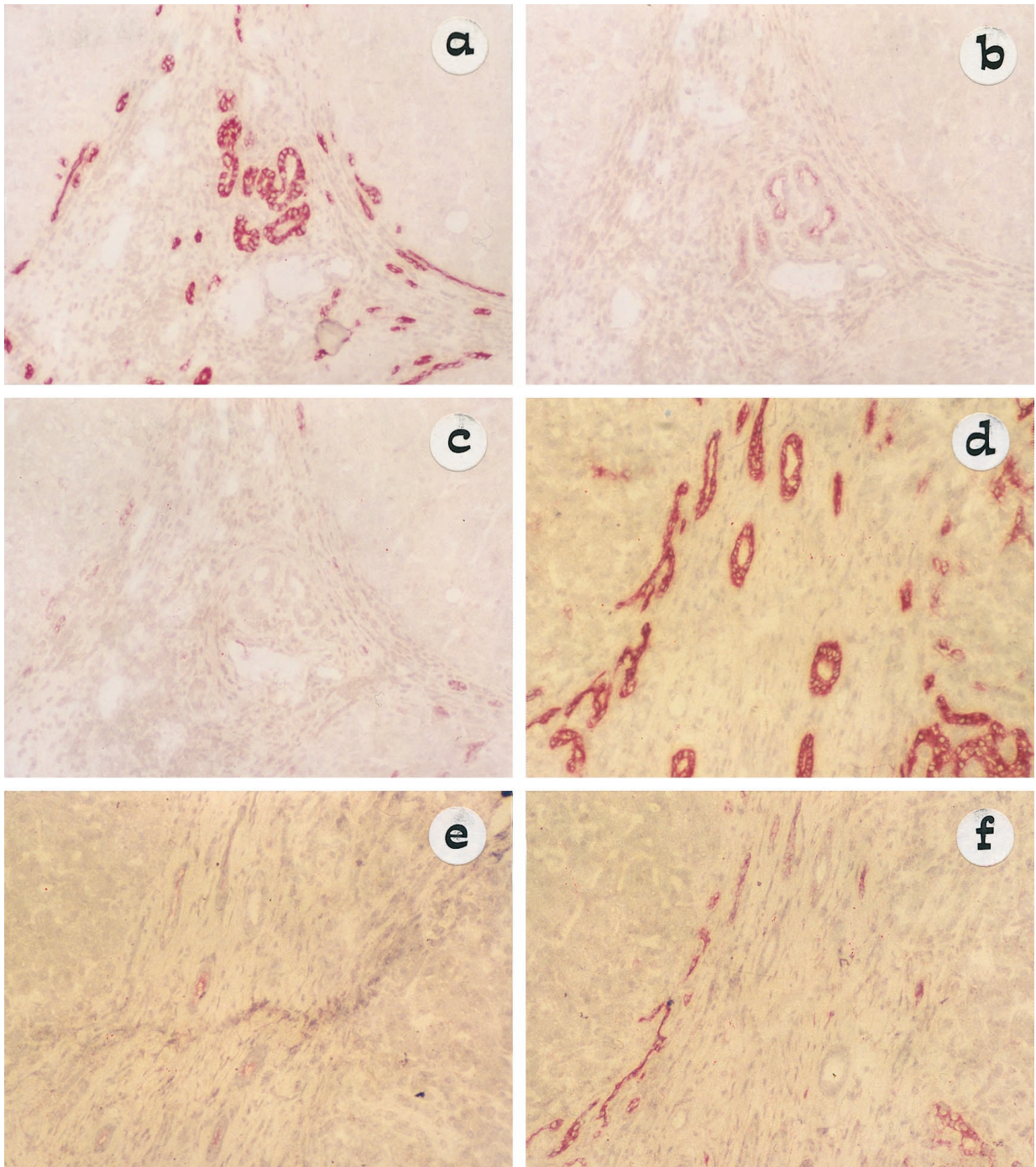


**Figure 2.** Light micrograph of single staining (APAAP method) showing the inverse relationship between EMA and NCAM expression on typical and atypical ductules, in alcoholic liver cirrhosis (**a–c**) and PSC (**d–f**) serial tissue sections (original magnification,  $\times 10$ ). HEA-125 has been used as marker of reference for biliary epithelium (**a** and **d**). EMA staining (apical localization) is positive in typical ductules at the center of the portal space and negative in the marginal atypical ductules (**b** and **e**), whereas NCAM decorates atypical but not typical ductules (**c** and **f**). Note the different extension of NCAM immunoreactivity on atypical ductules between alcoholic liver cirrhosis (**a** and **c**) and PSC (**d** and **f**).

### Cell Isolation

#### *Differential Immunomagnetic Purification of Immature versus Mature Biliary Epithelial Cells and Their Characterization by TEM*

Anti-NCAM antibody was used to purify atypical ductular cells from the Percoll fractions 2 and 3, which were

combined to increase the cell yield. The harvested cells were single cells or small aggregates composed of  $\sim 2$ – $10$  cells each and were positive also for HEA-125 and CK19, but were negative for EMA (not shown). Whereas NCAM-positive cells could be harvested from cirrhotic liver ( $10^3$  to  $10^4$  NCAM-positive cells/g of cirrhotic liver), none could be isolated from normal liver, thus reflecting the immunohistochemical finding. TEM demonstrated



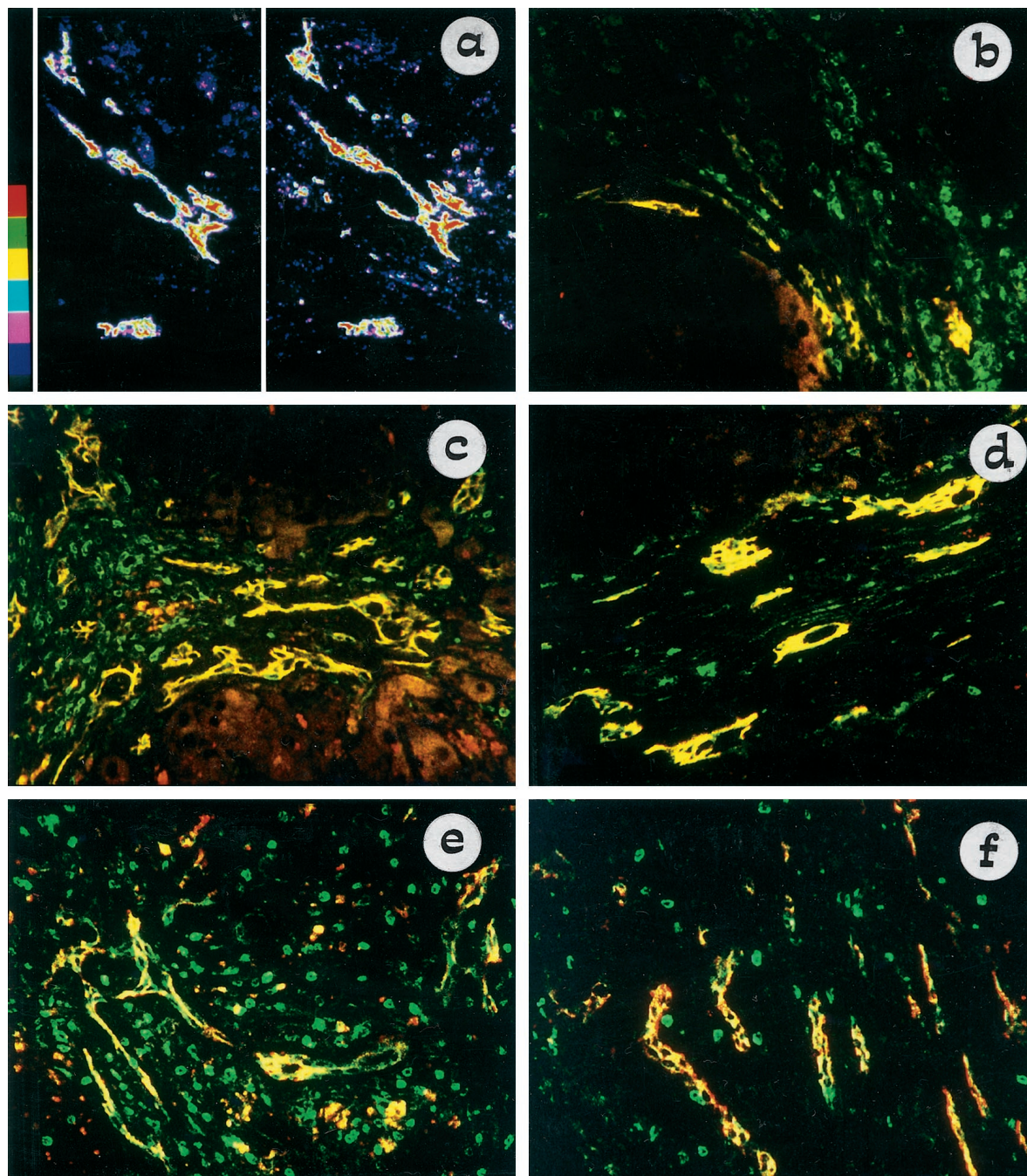


**Figure 3.** Confocal micrograph of double staining with NCAM (Texas Red) and Bcl-2 (FITC), showing coincident expression between these two markers on atypical ductules. In **a** the level of coincidence between NCAM (**left side**) and Bcl-2 (**right side**) is analyzed by dismerging and color banding in a biliary atresia tissue sample: the highest intensities are shown in red, and the lowest intensities are in blue. NCAM and Bcl-2 share the same distribution and concentration on biliary epithelium: the highest and the lowest levels of binding of NCAM and Bcl-2 are localized at the same places within the atypical ductular structures. All control reactions demonstrated the specificity of the double staining. In **b-f**, NCAM and Bcl-2 coexpression on ductular reaction is reported for different chronic hepatobiliary diseases: cryptogenic cirrhosis (**b**), PSC (**c**), biliary atresia (**d**), polycystic liver (**e**), and Caroli's disease (**f**). Areas of coincident labeling appear yellow. Bcl-2 noncoincident staining (green) is observed in lymphocytes. In parenchymal liver cirrhosis (**b**) only a small subset of reactive ductules, characterized by a marginal distribution, coexpressed NCAM and Bcl-2. In primary cholangiopathies (**c** and **d**) and developmental liver diseases related to ductal plate malformation (**e** and **f**), coincident immunoreactivity for NCAM and Bcl-2 was extensively observed among atypical ductules. In **c** granular NCAM staining (red) was found in scattered periportal hepatocytes.

that these cells were characterized by a rounded shape and a scant cytoplasm, showed only few short microvilli, had a poor intracellular organization, and lacked polarity (Figure 5a), consistent with an immature epithelial phenotype.

Mature biliary epithelial cells were purified from the same livers, using HEA-125 on the NCAM-depleted population after isolation of NCAM-positive ductular cells. In cirrhotic and normal livers this procedure yielded aggregates that generally were larger than those isolated with



**Table 3.** Proportion of NCAM-Positive Atypical Ductules in Different Forms of Chronic Liver Disease

Liver Disease	% of HEA-125-positive atypical ductuals expressing NCAM	
	Median	Range
Biliary atresia ( <i>n</i> = 2)	98	96–100
PBC ( <i>n</i> = 2)	86	80–90
PSC ( <i>n</i> = 1)	58	54–60
Cryptogenic cirrhosis ( <i>n</i> = 2)	26	18–30
Alcoholic cirrhosis ( <i>n</i> = 1)	35	20–58
Autoimmune hepatitis ( <i>n</i> = 1)	12	5–15

The number of tissue samples studied for the different forms of liver cirrhosis is given in parentheses. For each tissue sample at least three portal tracts were examined at random.

anti-NCAM: approximately 10–100 cells per aggregate, which were positive also for CK19 and EMA, but negative for NCAM (not shown). In contrast with the NCAM-positive fraction, TEM of these cells showed a cuboidal or columnar shape and a clear polar morphology: nuclei were situated at the basal region, and well-formed microvilli could be observed at the apical surface. The cytoplasm contained sparse mitochondria and a well-organized endoplasmic reticulum. Junctional complexes could be seen between adjacent cells (Figure 5b).

### Discussion

NCAM plays an important role in morphogenesis,<sup>26–29</sup> as documented in the nervous system, where neutralizing NCAM activity with monoclonal antibodies leads to altered morphology.<sup>45–47</sup> In addition to mediating homophilic and heterophilic cell interactions, NCAM may directly induce, for example, neurite development by stimulating the tyrosine kinase activity of fibroblast growth factor receptor in neighboring cells.<sup>48</sup> Roskams first observed NCAM expression on reactive bile ductules, together with other neuroendocrine features.<sup>24</sup> By comparing NCAM distribution to that of different immunophenotypic markers of cellular differentiation and proliferation in a wide variety of chronic liver diseases and in fetal livers from different gestational ages, our studies expand these early observations. Our data show that 1) atypical reactive ductules coexpress NCAM and Bcl-2 and are particularly represented in congenital diseases related to ductal plate malformation, in biliary atresia, and in immune-mediated primary cholangiopathies; 2) in fetal liver these markers are transiently expressed on biliary cells, during the early developmental stages of ductal plates, whereas 3) in liver diseases, NCAM/Bcl-2 identifies a biliary cell compartment, which shows a not fully differentiated epithelial phenotype. Finally, 4) using a positive

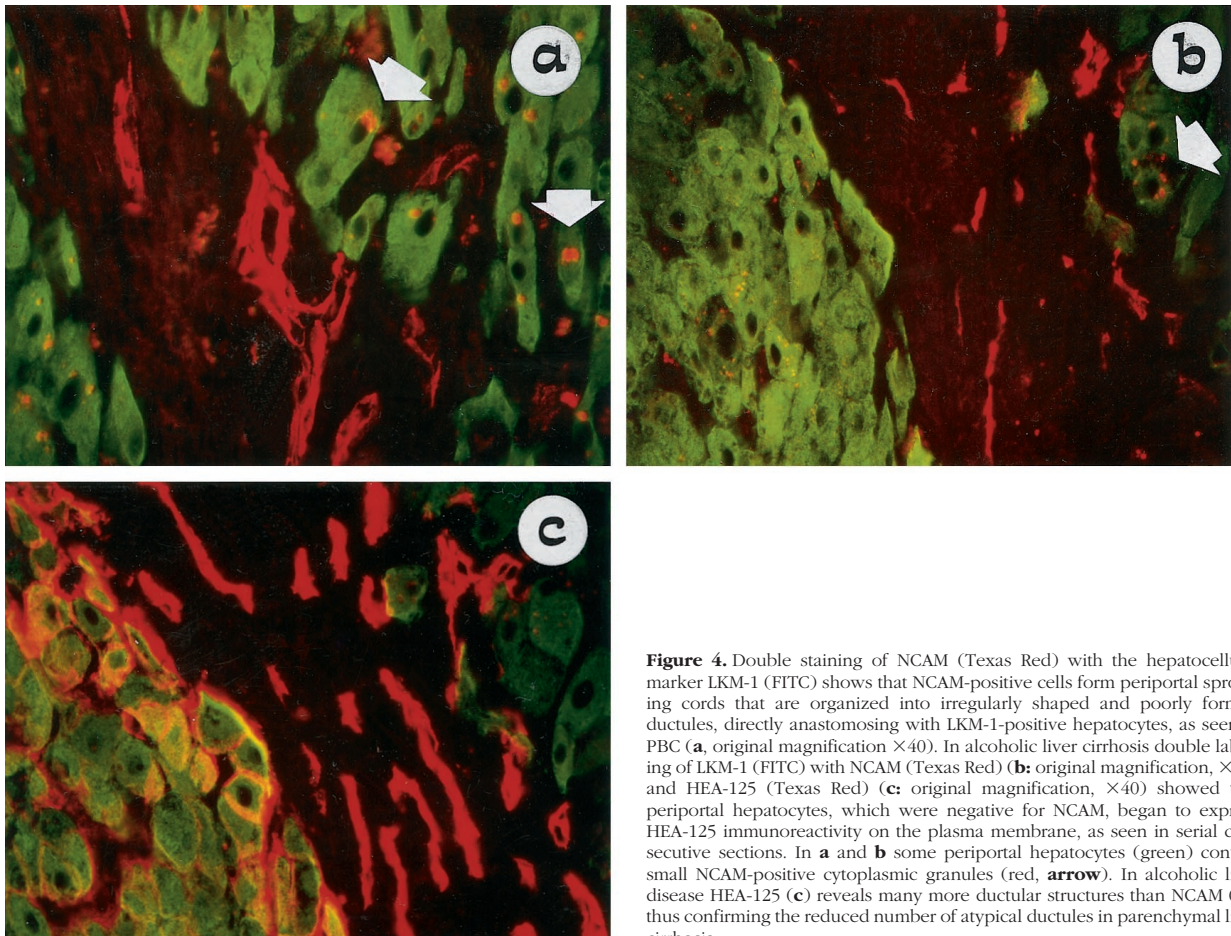


**Figure 4.** Double staining of NCAM (Texas Red) with the hepatocellular marker LKM-1 (FITC) shows that NCAM-positive cells form periportal sprouting cords that are organized into irregularly shaped and poorly formed ductules, directly anastomosing with LKM-1-positive hepatocytes, as seen in PBC (**a**, original magnification  $\times 40$ ). In alcoholic liver cirrhosis double labeling of LKM-1 (FITC) with NCAM (Texas Red) (**b**: original magnification,  $\times 40$ ) and HEA-125 (Texas Red) (**c**: original magnification,  $\times 40$ ) showed that periportal hepatocytes, which were negative for NCAM, began to express HEA-125 immunoreactivity on the plasma membrane, as seen in serial consecutive sections. In **a** and **b** some periportal hepatocytes (green) contain small NCAM-positive cytoplasmic granules (red, arrow). In alcoholic liver disease HEA-125 (**c**) reveals many more ductular structures than NCAM (**b**), thus confirming the reduced number of atypical ductules in parenchymal liver cirrhosis.

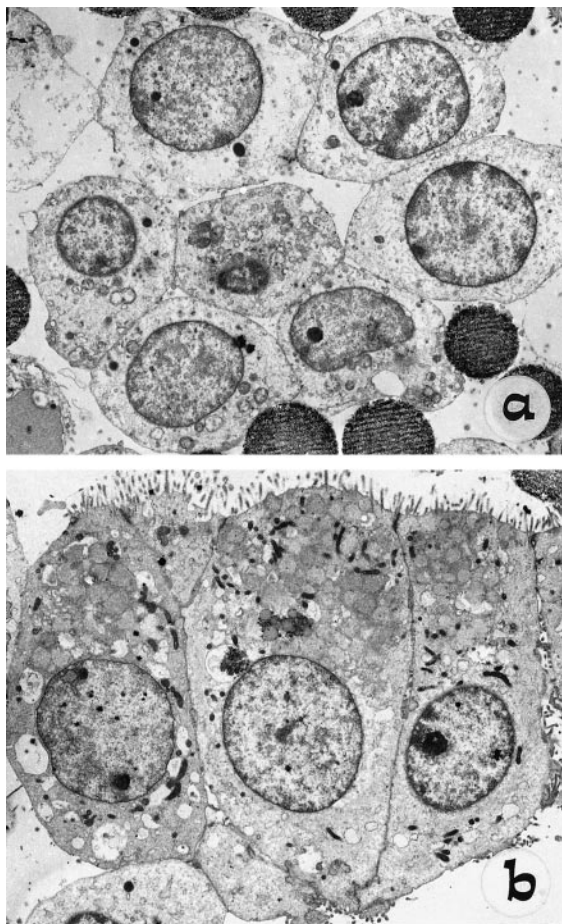


**Figure 5.** Ultrastructural analysis by TEM of cells freshly isolated from Percoll gradients by immunomagnetic separation, using anti-NCAM (**a**) and HEA-125 (**b**) on the NCAM-depleted population. Note the polar columnar morphology, with basal nuclei and well-formed apical microvilli of mature biliary epithelial cells (**b**), compared with the rounded shape, high nucleus-cytoplasmic ratio, short scattered microvilli, and fewer junctional complexes of NCAM-positive cells (**a**).

selection of cells expressing NCAM, we have devised a method for obtaining a highly pure and viable population of biliary cells with less differentiated ultrastructural features than mature cholangiocytes.

The normal biliary epithelium was homogeneously stained by HEA-125 and EMA, but was consistently negative for NCAM. In our hands Bcl-2 was not expressed on small ducts from normal livers, which is consistent with early reports from Frommel,<sup>49</sup> Arora,<sup>50</sup> and Gapany.<sup>51</sup> These findings are at odds with those reported by Charlotte<sup>52</sup> and Skopelitou.<sup>53</sup> Differences in the source of control tissue are likely the cause of these different findings. In Charlotte's study normal tissue was taken from hepatectomies performed for liver cancer, a source that may not be considered appropriate.<sup>54</sup> However, any uncertainty about whether bile ducts in normal liver are positive for Bcl-2 does not detract from our observation that NCAM-positive ductular cells in fetal and diseased liver were also Bcl-2-positive.

In fact, in contrast with normal biliary epithelium, NCAM and Bcl-2 were transiently expressed on immature biliary cells at a very early developmental stage of the

intrahepatic biliary tree (10th week); these cells, which were positive for HEA-125 but negative for EMA and Ki-67, were organized into a single-layered ductal plate, still lacking a lumen. Over the following weeks, when ductal plates duplicated and began to assume the shape of a tubular structure lining a slit-like circular lumen, they gradually lost NCAM and Bcl-2 expression, began to express EMA, and showed a proliferation activity. These data are consistent with those of Terada and Nakanuma,<sup>55</sup> who reported a relatively high rate of proliferation and apoptosis when ductal plates began to be incorporated into the mesenchyma (remodeling ductal plate). Conversely, the single-layered ductal plate showed poor evidence of active proliferation in Terada's study, as well as in our own. Negativity of ductal plate for proliferation markers at the 12th week has also been reported by Cocjin.<sup>56</sup> An intense proliferation activity was instead observed in hepatoblasts, consistent with the hypothesis that ductal plate is formed via a phenotypic shift from hepatoblasts to biliary cells.<sup>17,34</sup> Similar to the progressive expression of additional cytokeratin types (first CK-19 and then CK-7), NCAM, Bcl-2, and EMA may thus be considered as differentiation markers along the biliary cell lineage.

In reactive ductules from diseased livers, we have observed a pattern of expression similar to that found in fetal livers. In these conditions immunoreactivity for NCAM and Bcl-2 and negativity for EMA identified ductules with an atypical morphology. Instead, typical reactive ductules were positive for EMA, a marker of terminally differentiated biliary cells,<sup>57</sup> further indicating that typical ductules retain the phenotypic properties of their normal counterparts.<sup>58</sup> Ductules coexpressing NCAM and Bcl-2 were particularly represented in diseases of ductal plate malformation, such as polycystic liver disease and Caroli's disease. In these developmental liver diseases, ductal plate remodeling is arrested during the embryonic development, causing the persistence of an excess of bile ductules in a ductal plate configuration with immunophenotypic features of immaturity.<sup>59</sup> Similar to ductal plate malformations, in extrahepatic bile duct atresia and in immune-mediated cholangiopathies (PBC and PSC), most reactive ductules were positive for NCAM and Bcl-2 and were distributed throughout the portal tracts, whereas in parenchymal liver cirrhosis ductules that reacted with NCAM and Bcl-2 were much less represented and were confined to the interface between the portal space and the regenerative nodule. The different pattern of extension of NCAM reactivity on reactive ductules between cholestatic and parenchymal liver diseases (see Table 3 and Figures 2 and 3), particularly their wider distribution throughout the portal space in primary cholangiopathies, suggests that retention of bile constituents is a strong stimulus for atypical ductular reaction. Interestingly, in contrast with experimental bile duct ligation, where proliferation of preexisting biliary epithelial cells gives rise to well-differentiated bile ducts, under these conditions ductular structures appeared unable to form mature ducts.

The colocalization of NCAM with Bcl-2 in atypical ductules from diseased livers may be related to the role



**Table 4.** Differential Expression of Maturation Markers in Fetal and Adult Diseased Liver

Markers	Fetal liver (10–16 gestational weeks)			Adult diseased liver		
	Unduplicated ductal plate	Duplicated ductal plate	Hepatoblasts	Atypical ductules	Mature ducts	Periportal hepatocytes
CK7 <sup>17,34</sup>	–	–	–	+	+	+
CK8 <sup>17,34</sup>	+	+	+	+	+	+
CK18 <sup>17,34</sup>	+	+	+	+	+	+
CK19 <sup>17,34</sup>	+	+	+	+	+	±
HEA-125	+	+	+	+	+	+*
NCAM	+	Patchy	–	+	Rare	–
Bcl-2	+	Patchy	–	+	Rare	–
Ki-67	–	Rare	+	–	Rare	+
EMA	–	±	–	–	+	–
CD33 <sup>67</sup>	+	+	–	ND	ND	ND
CD34 <sup>67</sup>	+	+	–	ND	ND	ND
c-kit <sup>67</sup>	+	+	±	ND	ND	ND
OV-6 <sup>74–76</sup>	Patchy	Patchy	Scattered	Patchy	Patchy	+†

\*HEA-125-positive periportal hepatocytes were observed mainly in parenchymal liver cirrhosis (see text).

†OV-6-positive periportal hepatocytes were observed in PSC<sup>74</sup> and in biliary atresia and  $\alpha$ 1-anti-trypsin deficiency.<sup>75</sup>

of these two proteins in morphogenesis. NCAM is known to mediate the establishment of cell-cell and cell-matrix interactions<sup>26,27,60</sup>; homophilic and heterophilic interactions through NCAM are crucial to regulate the migration of cells and the differentiation of tissues in the embryo. For example, when neural crest cells stop producing NCAM and N-cadherin and start displaying integrin receptors, they can separate and begin to migrate on the extracellular matrix.<sup>61</sup> In a similar manner, in fetal livers, NCAM may play a role in mediating the phenotypic shift from hepatoblasts to ductal plate cells,<sup>17,34</sup> induced by the mesenchyme that surrounds the portal vein branches.<sup>62</sup> On the other hand, Bcl-2 may favor survival and clustering of immature cells that are committed to the formation of more differentiated structures.<sup>31</sup> Bcl-2 is known to be expressed in several fetal tissues (skin, tracheobronchial tree, kidney), at sites characterized by inductive interactions between epithelial and mesenchymal structures, and it may play a role not only in blocking apoptosis (a major mechanism in tissue remodeling) but also in the commitment process of cells engaged in the formation of new structures.<sup>31,32</sup> Thus coexpression of NCAM and Bcl-2 on “atypical” ductules after chronic liver damage is likely induced by changes in extracellular matrix and identifies immature biliary cells with prolonged survival advantage, because they are involved in active tissue remodeling processes.

Our data indicate that, in contrast to periportal hepatocytes, atypical reactive ductules coexpressing NCAM and Bcl-2 were not actively proliferating, as shown by negative double labeling of NCAM with Ki-67. These expression patterns resemble those seen early in developing ductal plates from 10 to 16 gestation weeks. Early Bcl-2 expression is a well-documented event in the process of metaplasia, as reported in Barrett esophagus<sup>63</sup> and gastric intestinal metaplasia.<sup>64</sup> In particular, in gastric intestinal metaplasia double staining for Bcl-2 and Ki-67 revealed that Bcl-2 was not expressed by proliferating epithelial cells, but was present in cells undergoing metaplasia,<sup>64</sup> as reported here for NCAM-positive atypical ductular cells. By the use of computerized three-

dimensional reconstructions of the biliary system, atypical ductules were shown to be in communication with liver cell plates but not with preexisting bile ducts and ductules.<sup>65</sup> Both the flattened shape and the network arrangement of atypical ductules are difficult to explain as a result of proliferation of preexisting ducts and are more consistent with an origin in liver cell muralia<sup>66</sup> or cells located at the canal of Hering. This hypothesis is further supported by double staining of NCAM with the hepatocellular marker LKM-1. In all types of liver disease studied, NCAM-positive atypical ductules appeared to be in close proximity to LKM-1-positive hepatocytes at the margin of the portal tracts; immunoreactivity for NCAM was present in the cytoplasm of some periportal hepatocytes, but cells coexpressing LKM-1 and NCAM on the plasma membrane were not observed. In parenchymal liver cirrhosis, and particularly in alcoholic liver disease, double staining with HEA-125 and LKM-1 revealed a coincident labeling in some periportal hepatocytes, but these structures were negative for NCAM, indicating that NCAM expression is associated with loss of hepatocellular phenotype.

Thus, ductular reactive cells, protected from apoptotic events, but not actively proliferating, express neuroendocrine features, including immunoreactivity for NCAM; some of these features are reminiscent of the early phases of biliary ontogenesis. There are a number of similarities and differences between ductal plate cells and ductular cells, and these are emphasized in Table 4. A major difference is that in ductular reaction CK7 appears in metaplastic hepatocytes before the expression of CK19,<sup>17,34</sup> a sequence of events opposite that observed during embryogenesis of biliary epithelium that first expresses CK19 and later CK7. Furthermore, it is unknown whether atypical reactive ductules express the hematopoietic stem cell markers CD34, CD33, and c-kit, the expression of which on ductal plate cells during the early stages of the embryonic development has been reported.<sup>67</sup>

Thus NCAM is not a marker of stem or bipotential cells; rather it is expressed in cells that are already committed

to the biliary lineage, although they are not fully differentiated. The contention that NCAM expression identifies biliary cells that are not fully differentiated is also supported by the ultrastructural appearance of freshly isolated NCAM-positive cells. When compared to mature biliary epithelial cells isolated from the same liver, NCAM-positive cells were single cells or small clumps (2–10 cells for aggregate), and by electron microscopic examination they showed a rounded shape with a high nucleus-cytoplasmic ratio, short stubby microvilli spread along the surface, fewer junctional complexes between adjacent cells, and low amounts of mitochondria and rough endoplasmic reticulum, consistent with an immature phenotype lacking a polar organization. This interpretation is also supported by the lack of the mature cholangiocyte marker EMA, by the negativity of NCAM staining on mature bile ducts, and by the transient expression of NCAM in fetal livers. Although less differentiated than mature cholangiocytes, NCAM-positive cells show no evidence of active proliferation. Similarly, cells from the single-layered ductal plate were also negative for proliferation markers. Conversely, hepatoblasts in fetal livers and periportal hepatocytes in chronic liver diseases were both strongly positive for Ki-67.

Thus the data support the concept that atypical ductular reaction in chronic liver diseases recapitulates a program similar to the early stages of biliary ontogenesis, when NCAM-positive ductal plate cells are formed by hepatoblasts undergoing a phenotypic switch. Thus, as proposed by Van Eyken,<sup>68</sup> ductular reactive cells may derive from a ductular metaplasia of periportal hepatocytes. In fact, in addition to the so-called single-step or direct metaplasia, involving the direct switch of one overtly differentiated cell type to another, metaplasia may also occur as a multistep process. This is characterized by the appearance of intermediate cells, which possess a less differentiated phenotype but are committed to a different cell lineage (indirect metaplasia).<sup>68–70</sup> NCAM-positive ductal plate cells in embryogenesis and NCAM-positive ductules in chronic liver diseases may be the intermediate cells (hepatoblasts → NCAM-positive ductal plate cells → mature cholangiocyte). Our data do not exclude the presence of liver stem cell or a role for liver stem cells in generating the cells that ultimately become NCAM-positive ductules and, later, mature duct cells. From this point of view, the less differentiated characteristics and the lack of proliferation activity of the ductular cells coexpressing NCAM and Bcl-2 are consistent with the possibility they are the descendants of a small progenitor cell compartment, which could persist in the postnatal liver in close proximity to the finest ramifications of the biliary tree. Whether these progenitor cells give rise to periportal hepatocyte-like cells that may differentiate in hepatocytes and/or in biliary cells, or whether the progenitor cell itself differentiates directly either into hepatocytes or bile duct cells cannot be addressed in the present study. It is interesting to note that, as already reported for hepatoblasts,<sup>71</sup> in diseased livers (see Figure 4c) periportal hepatocytes are positive for the cholangiocyte marker HEA-125, an epithelial cell surface antigen homologous to the matrix adhesion protein nidogen.<sup>72</sup> In

chronic cholestatic liver disease, maturation of NCAM-positive ductular cells seems hampered, leading to the accumulation of less differentiated atypical ductules accompanied by the progressive disappearance of mature ducts that cannot be replaced (as seen, for example, in biliary atresia).

Regardless of their cell origin, the potential of these reactive ductular cells remains of great relevance. In fact, the ability to purify two subpopulations of immature and mature ductular cells is a novel technique that is likely to have an important impact on the study of biliary cell pathophysiology. This method will make it possible to study the role of reactive ductular cells in the production of several paracrine factors involved in regenerative and fibrotic processes, and to clarify the effects of different matrices on the growth properties and differentiation potential of these cells.

### Acknowledgments

The authors are grateful to Mrs. Ann Williams and Drs. Marcus Auth and Takaharu Sadamoto (Liver Research Laboratories, University of Birmingham) for the skillful technical assistance with the preparation of histological samples and help in cell isolations. We are also indebted to Dr. Gerald Johnson (Department of Immunology, University of Birmingham) for his expert advice regarding confocal analysis. Mrs. Leslie Tomkins and Mr. Peter Whittle (Department of Biochemistry, University of Birmingham) are acknowledged for preparations of TEM cell samples. Prof. Lajos Okolicsanyi (Chair of Gastroenterology, University of Parma), Dr. Paola Brun (Department of Biology, University of Padova), Dr. Mattia Quarta (Department of Medical and Surgical Sciences, University of Padova), and Dr. Mosè Favarato (Molecular Biology Laboratory, Hospital of Noale, Venice) are acknowledged for valuable suggestions and comments. Dr. Sabrina Ghetti (Policlinico S. Orsola, Bologna) is acknowledged for her help with the immunostaining experiments.

### References

1. Popper H, Schaffner F, Stein R: Ductular cell reaction in the liver in hepatic injury. *J Mt Sinai Hosp* 1957, 24:551–556
2. Masuko K, Rubin E, Popper H: Proliferation of bile ducts in cirrhosis. *Arch Pathol* 1964, 78:421–431
3. Desmet VJ, Roskams T, Van Eyken P: Ductular reaction in the liver. *Pathol Res Pract* 1995, 191:513–524
4. Roskams T, Rosenbau J, De Vos R, David G, Desmet VJ: Heparan sulfate proteoglycan expression in chronic cholestatic human liver diseases. *Hepatology* 1996, 24:524–532
5. Matsumoto K, Fuji H, Michalopoulos G, Fung JJ, Demetris AJ: Human biliary epithelial cells secrete and respond to cytokines and hepatocyte growth factors in vitro: interleukin-6, hepatocyte growth factor and epidermal growth factor promote DNA synthesis in vitro. *Hepatology* 1994, 20:376–382
6. Yasoshima M, Kono N, Sugawara H, Katayanagi K, Harda K, Nakanuma Y: Increased expression of interleukin-6 and tumor necrosis factor- $\alpha$  in pathologic biliary epithelial cells: in situ and culture study. *Lab Invest* 1998, 78:89–100
7. Milani S, Herbst H, Schuppan D, Stein H, Surrenti C: Transforming growth factor  $\beta$ 1 and  $\beta$ 2 are differentially expressed in fibrotic liver disease. *Am J Pathol* 1991, 139:1221–1229
8. De Groen PC, Vroman B, LaRusso NF: Physiologic regulation of



- cholangiocyte proliferation in vitro. Proceeding of the Digestive Disease Week 1996, May 19–22, San Francisco, CA
9. Marra F, De Franco R, Grappone C, Pinzani M, Milani S, Pastacaldi S, Laffi G, Gentilini P: Expression of monocyte chemotactic protein-1 during active hepatic fibrogenesis in humans. *Ital J Gastroenterol* 1996, 20:300–306
  10. Adams DH: Biliary epithelial cells: innocent victims or active participants in immuno-mediated liver diseases? *J Lab Clin Med* 1996, 128:528–530
  11. Berg PA, Klein R, Rocken M: Cytokines in primary biliary cirrhosis. *Semin Liver Dis* 1997, 17:115–123
  12. Vos TA, Gouw ASH, Klok PA, Havinga R, Van Goor H, Huitema S, Roelofsens H, Kuipers F, Jansen PLM, Moshage H: Differential effects of nitric oxide synthase inhibitors on endotoxin-induced liver damage in rats. *Gastroenterology* 1997, 113:1323–1333
  13. Roskams T, Campos RV, Drucker DJ, Desmet VJ: Reactive human bile ductules express parathyroid hormone-related peptide. *Histopathology* 1993, 23:11–19
  14. Sirica AE: Ductular hepatocytes. *Histol Histopathol* 1995, 10:433–456
  15. Sell S: Comparison of liver progenitor cells in human atypical ductular reactions with those seen in experimental models of liver injury. *Hepatology* 1998, 27:317–331
  16. Slott PA, Liu MJ, Tavoloni N: Origin, pattern and mechanism of bile duct proliferation following biliary obstruction in the rat. *Gastroenterology* 1990, 99:466–477
  17. Van Eyken P, Desmet VJ: Development of intrahepatic bile ducts, ductular metaplasia of hepatocytes, and cytokeratin expression in various types of human hepatic neoplasms. *The Role of Cell Types in Hepatocarcinogenesis*. Edited by AE Sirica. Boca Raton, FL, CRC Press, 1992, pp 227–263
  18. Fausto N: Liver stem cells. *The Liver: Biology and Pathobiology*. Edited by IM Arias, JL Boyer, N Fausto, WB Jakoby, DA Schachter, DA Shafritz. New York, Raven Press, 1994, pp 1501–1518
  19. Rouger P, Poupon R, Gane P, Mallissen B, Darnis F, Salmon C: Expression of blood group antigens including HLA markers in human adult liver. *Tissue Antigens* 1986, 27:78–86
  20. Nakanuma Y, Sasaki M: Expression of blood group-related antigens in the intrahepatic biliary tree and hepatocytes in normal livers and various hepatobiliary diseases. *Hepatology* 1989, 10:174–178
  21. Gerber MA, Thung SN, Shen S, Stromeyer FW, Ishak KG: Phenotypic characterization of hepatic proliferation: antigenic expression by proliferating epithelial cells in fetal liver, massive hepatic necrosis, and nodular transformation of the liver. *Am J Pathol* 1983, 110:70–74
  22. Adams DH, Hubscher SG, Shaw J, Johnson GD, Babbs C, Rothlein R, Neuberger JM: Increased expression of intercellular adhesion molecule 1 on bile ducts in primary biliary cirrhosis and primary sclerosing cholangitis. *Hepatology* 1991, 14:426–431
  23. Dillon P, Belchis D, Tracy T, Cilley R, Hafer L, Krummel T: Increased expression of intercellular adhesion molecules in biliary atresia. *Am J Pathol* 1994, 145:263–267
  24. Roskams T, Van den Oord JJ, De Vos R, Desmet VJ: Neuroendocrine features of reactive bile ductules in cholestatic liver disease. *Am J Pathol* 1990, 137:1019–1025
  25. McClain DA, Edelman GM: A neural cell adhesion molecule from human brain. *Proc Natl Acad Sci USA* 1982, 79:6380–6384
  26. Hoffman S, Edelman GM: Kinetics of homophilic binding by embryonic and adult forms of the neural cell adhesion molecule. *Proc Natl Acad Sci USA* 1983, 80:5762–5766
  27. Werz W, Schachner M: Adhesion of neural cells to extracellular matrix constituents. Involvement of glycosaminoglycans and cell adhesion molecules. *Dev Brain Res* 1988, 43:225–234
  28. Lanier LL, Testi R, Bindl J, Phillips JH: Identity of Leu-19 (CD 56) leukocyte differentiation antigen and neural cell adhesion molecule. *J Exp Med* 1989, 169:2233–2238
  29. Edelman GM, Crossin KL: Cell adhesion molecules: implications for a molecular histology. *Annu Rev Biochem* 1991, 60:155–190
  30. Hockenbery DM, Nunez G, Millman C, Schreiber RD, Korsmeyer SJ: Bcl-2 is an inner mitochondrial membrane protein that blocks programmed cell death. *Nature* 1990, 348:334–336
  31. Lu Q-L, Poulosom R, Wong L, Hanby AM: *BCL-2* expression in adult and embryonic non-haematopoietic tissues. *J Pathol* 1993, 169:431–437
  32. LeBrun DP, Warnke RA, Cleary ML: Expression of *bcl-2* in fetal tissues suggests a role in morphogenesis. *Am J Pathol* 1993, 142:743–753
  33. Ludwig J: New concepts in biliary cirrhosis. *Semin Liver Dis* 1987, 7:293–301
  34. Van Eyken P, Sciot R, Callea F, Van der Steen K, Moerman P, Desmet VJ: The development of the intrahepatic bile ducts in man: a keratin-immunohistochemical study. *Hepatology* 1988, 8:1586–1595
  35. Shah KD, Gerber MA: Development of intrahepatic bile ducts in humans. *Arch Pathol Lab Med* 1990, 114:597–600
  36. Hall PA, Levison DA: Review: assessment of cell proliferation in histological material. *J Clin Pathol* 1990, 43:184–192
  37. Johnson GD, Walker L: Reversed sequential double immunostaining—an indirect (antiglobulin) method for identifying cellular subsets using monoclonal antibodies of the same isotype. *J Immunol Methods* 1986, 95:149–152
  38. Ballardini G, Landi P, Busachi GA, Bianchi FB, Pisi E: HBsAg-induced hypertrophic smooth endoplasmic reticulum as a target for liver-kidney microsomal (LKM) antibodies. *Clin Exp Immunol* 1981, 43:599–604
  39. Bianchi FB, Biagini G, Ballardini G, Cenacchi G, Faccani A, Pisi E, Laschi R, Liotta L, Garbisa S: Basement membrane production by hepatocytes in chronic liver disease. *Hepatology* 1984, 4:1167–1172
  40. Homberg JC, Abuaf N, Bernard O, Islam S, Alvarez F, Khalil SH, Poupon R, Darnis F, Lévy VG, Gripon P, Opolon P, Bernuau J, Benhamou JP, Alagille D: Chronic active hepatitis associated with antiliver/kidney microsome antibody type 1: a second type of “auto-immune” hepatitis. *Hepatology* 1987, 7:1333–1339
  41. Manns MP, Griffin KJ, Sullivan KF, Johnson EF: LKM-1 autoantibodies recognize a short linear sequence in P450IID6, a cytochrome P-450 monooxygenase. *J Clin Invest* 1991, 88:1370–1378
  42. Momburg F, Moldenhauer G, Hammerling GH, Moller P: Immunohistochemical study of the surface expression of a  $M_r$  34,000 human epithelium-specific glycoprotein in normal and malignant tissues. *Cancer Res* 1987, 47:2883–2891
  43. Joplin R, Strain AJ, Neuberger JM: Immuno-isolation and culture of biliary epithelial cells from normal human liver. *In Vitro Cell Dev Biol* 1989, 25:1189–1192
  44. Joplin R, Strain AJ, Neuberger JM: Biliary epithelial cells from the liver of patients with primary biliary cirrhosis: isolation, characterization, and short-term culture. *J Pathol* 1990, 162:255–260
  45. Hoffman S, Friedlander DR, Chuong C-M, Grumet M, Edelman GM: Differential contributions of Ng-CAM and N-CAM to cell adhesion in different neural regions. *J Cell Biol* 1986, 103:145–158
  46. Fraser SE, Murray BA, Chuong C-M, Edelman GM: Alterations of the retinotectal map in *Xenopus* by antibodies to neural cell adhesion molecules. *Proc Natl Acad Sci USA* 1984, 81:4222–4226
  47. Buskirk DR, Thiery J-P, Rutishauser U, Edelman GM: Antibodies to a neural cell adhesion molecule disrupt histogenesis in cultured chick retinae. *Nature* 1980, 285:488–489
  48. Walsh FS, Doherty P: Neural cell adhesion molecules of the immunoglobulin superfamily: role in axon growth guidance. *Annu Rev Cell Dev Biol* 1997, 13:425–456
  49. Frommel TO, Yong S, Zarling EJ: Immunohistochemical evaluation of Bcl-2 gene family expression in liver of hepatitis C and cirrhotic patients: a novel mechanism to explain the high incidence of hepatocarcinoma in cirrhotics. *Am J Gastroenterol* 1999, 94:178–182
  50. Arora DS, Ramsdale J, Lodge JP, Wyatt JL: p53 but not bcl-2 is expressed by most cholangiocarcinomas: a study of 28 cases. *Histopathology* 1999, 34:497–501
  51. Gapany C, Zhao M, Zimmermann A: The apoptosis protector, bcl-2 protein, is downregulated in bile duct epithelial cells of human liver allografts. *J Hepatol* 1997, 26:535–542
  52. Charlotte F, L’Herminé A, Martin N, Geleyn Y, Nolle M, Gaulard P, Zafrani ES: Immunohistochemical detection of *bcl-2* protein in normal and pathological human liver. *Am J Pathol* 1994, 144:460–465
  53. Skopelitou A, Hadjiyannakis M, Alexopoulou V, Krikoni O, Kamina S, Agnantis N: Topographical immunohistochemical expression of bcl-2 protein in human liver lesions. *Anticancer Res* 1996, 16:975–978
  54. Venturi C, Bortolami M, Farinati F, Carlotto C, Scalera R: Can unaffected areas surrounding liver tumors be considered as “normal”? *Hepatology* 1996, 24:346A
  55. Terada T, Nakanuma Y: Detection of apoptosis and expression of apoptosis-related proteins during human intrahepatic bile duct development. *Am J Pathol* 1995, 146:67–74
  56. Cocjin J, Rosenthal P, Buslon V, Luk L Jr, Barajas L, Geller SA, Ruebner B, French S: Bile ductule formation in fetal, neonatal, and

- infant livers compared with extrahepatic biliary atresia. *Hepatology* 1996, 24:568–574
57. Delladetsima JK, Kyriakou V, Vafiadis I, Karakitsos P, Smyrnof T, Tassopoulos NC: Ductular structures in acute hepatitis with panacinar necrosis. *J Pathol* 1995, 175:69–76
  58. Nakanuma Y, Ohta G: Immunohistochemical study on bile ductular proliferation in various hepatobiliary diseases. *Liver* 1986, 6:205–211
  59. Desmet VJ: Congenital disease of intrahepatic bile ducts: variations on the theme "ductal plate malformation." *Hepatology* 1992, 16:1069–1083
  60. Gumbiner BM: Cell adhesion: the molecular basis of tissue architecture and morphogenesis. *Cell* 1996, 84:345–357
  61. Ruoslahti E: Control of cell motility and tumor invasion by extracellular matrix interactions. *Br J Cancer* 1992, 66:239–242
  62. Amenta PS, Harrison D: Expression and potential role of the extracellular matrix in hepatic ontogenesis: a review. *Microsc Res Tech* 1997, 39:372–386
  63. Katada N, Hinder RA, Smyrk TC, Hirabayashi N, Perdakis G, Lund R, Woodward T, Klingler PJ: Apoptosis is inhibited early in the dysplasia-carcinoma sequence of Barrett esophagus. *Arch Surg* 1997, 132:728–733
  64. Saegusa M, Takano Y, Okayasu I: Bcl-2 expression and its association with cell kinetics in human gastric carcinomas and intestinal metaplasia. *J Cancer Res Clin Oncol* 1995, 121:357–363
  65. Yamada S, Howe S, Scheuer PJ: Three-dimensional reconstruction of biliary pathways in primary biliary cirrhosis: a computer-assisted study. *J Pathol* 1987, 152:317–323
  66. Jorgensen M: A stereological study of intrahepatic bile ducts. 2. Bile duct proliferation in some pathological conditions. *Acta Pathol Microbiol Scand A* 1973, 81:663–669
  67. Blakolmer K, Jaskiewicz K, Dunsford HA, Robson SC: Hematopoietic stem cell markers are expressed by ductal plate and bile duct cells in developing human liver. *Hepatology* 1995, 21:1510–1516
  68. Van Eyken P, Desmet VJ: Ductular metaplasia of hepatocytes. *Biliary and Pancreatic Duct Epithelia*. Edited by AE Sirica, DS Longnecker. New York, Basel, Hong Kong, Dekker, 1997, pp 201–228
  69. Lugo M, Plutong PB: Metaplasia: an overview. *Arch Pathol Lab Med* 1984, 108:185–189
  70. Slack JMW: Epithelial metaplasia and the second anatomy. *Lancet* 1986, 2:268–270
  71. Crosby HA, Hubscher SG, Joplin RE, Kelly DA, Strain AJ: Immunolocalization of OV-6, a putative progenitor cell marker in human fetal and diseased pediatric liver. *Hepatology* 1998, 28:980–985
  72. Simon B, Podolsky DK, Moldenhauer G, Issebacher KJ, Gattoni-Celli S, Brand SJ: Epithelial glycoprotein is a member of a family of epithelial cell surface antigens homologous to nidogen, a matrix adhesion protein. *Proc Natl Acad Sci USA* 1990, 87:2755–2759